Karlsruhe Institute of Technology

Non-factorisable contribution to t-channel single-top production

Based on arXiv:2204.05770 with Christian Brønnum-Hansen, Kirill Melnikov, Chiara Signorile-Signorile & Chen-Yu Wang

Jérémie Quarroz | 7th June 2022 | Orsay

Motivation

- Top quark is the heaviest particle of the Standard Model.
  - ➥ Better understanding of electroweak symmetry breaking.
  - ➥ Hopefully, hints for physics beyond the Standard Model.

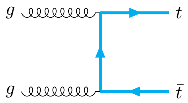

- Primarily produced in pairs. However, **single-top** production also occurs frequently

$$\sigma_{t,\text{single}} \approx \frac{1}{4}\sigma_{t\bar{t}}$$

- tWb interaction is interesting due to:
  - ➥ determination of the CKM matrix element V_{bt}
  - ➥ indirect determination of Γ_t and the top-quark mass m_t
  - ➥ constrains on bottom-quark PDF $f_b(x_1)$

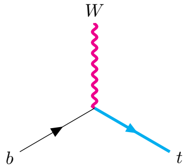

Single-top production

There are three single-top production modes

t channel: $qb \to q' t$

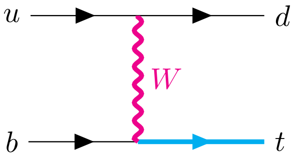

$\mathcal{O}$ (70%)

associated production:
$gb \to Wt$

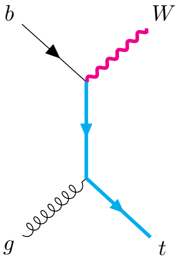

$\mathcal{O}$ (25%)

s channel: $q\bar{q}' \to W^* \to t\bar{b}$

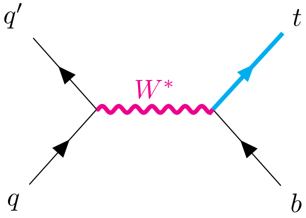

$\mathcal{O}$ (5%)

The main production mode is the t-channel.

NNLO QCD corrections to t-channel single-top production

Higher order corrections are known up to an advanced stage.

- NLO QCD and electroweak corrections are known since a while. *Harris et al. 2002; Campbell, Ellis, et al. 2004; Sullivan 2004; Cao and Yuan 2005; Sullivan 2005; Beccaria et al. 2006; Schwienhorst et al. 2011*
- NNLO QCD corrections are known **except for non-factorisable corrections**. *Brucherseifer, Caola and Melnikov 2014; Berger, Edmond, Gao, Yuan, Zhu 2016; Campbell, Neumann and Sullivan 2021*

Factorisable

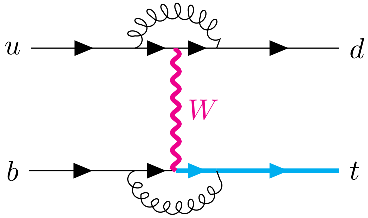

Non-factorisable

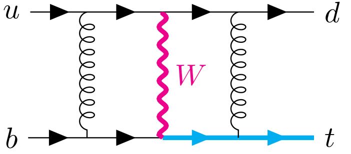

Factorisable approximation

These *non-factorisable* corrections are **colour-suppressed** and, therefore, are expected to be **negligible**.

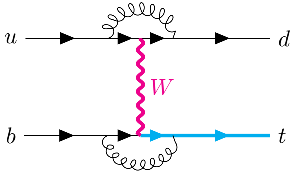

$$\mathrm{tr}\left(t^a t^a\right)\mathrm{tr}\left(t^b t^b\right) = \frac{1}{4}(N_c^2 - 1)^2$$

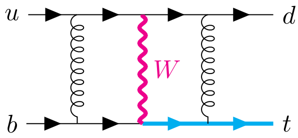

$$\mathrm{tr}\left(t^a t^b\right)\mathrm{tr}\left(t^a t^b\right) = \frac{1}{4}(N_c^2 - 1)$$

Non-factorisable corrections **vanish** at NLO because of colour.

→ **No indication from NLO.**

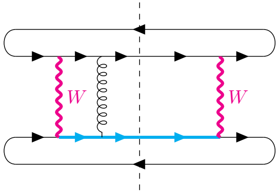

$\propto \mathrm{Tr}[t^a] = 0$

Non-factorisable contributions

However, it is not obvious that *non-factorisable* corrections are in fact negligible.

- Factorisable NNLO QCD corrections are **small** (few %).
- **Possible π^2 enhancement** due to the *Glauber phase*.
  - ➥ **Virtual effect** that, in principle, does not require a scattering to occur. $p_\perp^t \to 0$

$$\sigma = \underbrace{\sigma_0 + \overbrace{\frac{p_\perp^t}{\sqrt{s}}\,\sigma_1 + \mathcal{O}\left(\left(p_\perp^t/\sqrt{s}\right)^2\right)}^{\text{real emission}}}_{\text{virtual correction}} \qquad p_\perp^t \sim 40\,\mathrm{GeV} \qquad \sqrt{s} \sim 300\,\mathrm{GeV}$$

($\pi^2 \to \sigma_0$)

  - ➥ Explicitely proved for the non-factorisable corrections to the Higgs production in weak boson fusion in the eikonal approximation. *Liu, Melnikov, et al. 2019*

This factor $\pi^2 \sim 10$ could **compensate** the factor 8 from colour suppression.

A better understanding of **non-factorisable** corrections to single-top production at LHC would be **beneficial**.

Purposes of this work

$\mathcal{A}_6^{(0)} =$

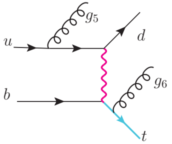

$\mathcal{A}_5^{(1)} =$

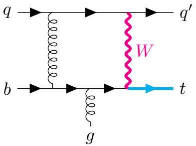

To calculate the non-factorisable corrections to single-top production.

$$d\hat{\sigma}^{\rm NNLO}_{\rm n.f.} = \underbrace{d\hat{\sigma}_{\rm RR}}_{\mathcal{A}_6^{(0)}} + \underbrace{d\hat{\sigma}_{\rm RV}}_{\mathcal{A}_5^{(1)},\,\mathcal{A}_5^{(0)}} + \underbrace{d\hat{\sigma}_{\rm VV}}_{\mathcal{A}_4^{(2)},\,\mathcal{A}_4^{(1)},\,\mathcal{A}_4^{(0)}}$$

- We keep the **exact dependence** on kinematic invariants, m_t and m_W.
- Master two-loop integrals are computed using the **auxiliary mass flow method**. *Liu, Ma, and Wang 2018*

$\mathcal{A}_4^{(2)} =$

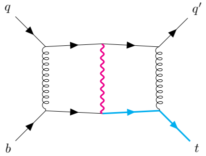

$\mathcal{A}_4^{(1)} =$

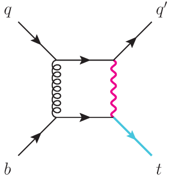

Properties of the process

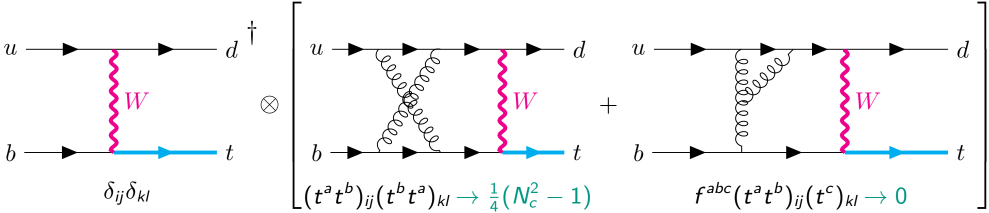

Upon interference, the non-Abelian part of the amplitude disappears and the amplitude is, effectively, **Abelian**.

UV and IR singularities

- Non-factorisable contributions are **UV-finite** at NNLO.

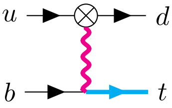

$\delta_{ij}\delta_{kl}$

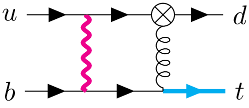

$t^a_{ij}t^a_{kl}$

- **No collinear singularities** appear in non-factorisable contributions

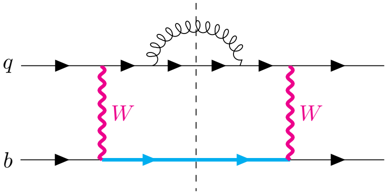

$\in$ factorisable corrections

All singularities are from soft origin.

IBP reduction

- Reduction performed **analytically** with KIRA 2.0: *Klappert, Lange, et al. 2020* and FireFly *Klappert and Lange 2020; Klappert, Klein, et al. 2021:*

$$\langle \mathcal{A}^{(0)} | \mathcal{A}_{\text{nf}}^{(2)} \rangle = \frac{1}{4}(N_C^2 - 1) \sum_{i=1}^{428} c_i(d, s, t, m_t, m_W) I_i$$

- 428 master integrals I_i in 18 families

1st planar family

$$D_i \in \Big\{ k_1^2,\ (k_1 - p_1)^2, (k_1 + p_2)^2, (k_2 + p_3)^2, (k_1 + k_2 - p_1 + p_3)^2, (k_2 - p_1 - p_2 + p_3)^2, k_2^2 - m_W^2, k_1 \cdot p_3,\ k_2 \cdot p_2 \Big\}$$

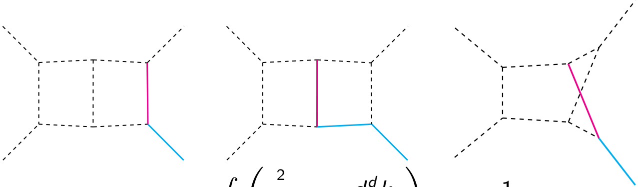

$$I(a_1, \ldots, a_9) = \int \left(\prod_{n=1}^{2} e^{\epsilon \gamma_E} \frac{d^d k_n}{i\pi^{d/2}} \right) \frac{1}{D_1^{a_1} D_2^{a_2} \ldots D_9^{a_9}}$$

Master integrals evaluation

- Based on the **auxiliary mass flow method** *Liu, Ma, and Wang 2018; Liu, Ma, Tao, et al. 2020; Liu and Ma 2021*

$$I \propto \lim_{\eta \to 0^+} \int \prod_{i=1}^{2} \mathrm{d}^d k_i \prod_{a=1}^{9} \frac{1}{[q_a^2 - (m_a^2 - i\eta) + i\epsilon]^{\nu_a}}$$

- Add an imaginary part to the W **boson mass**

$$m_W^2 \to m_W^2 - i\eta.$$

- Solve differential equations at each kinematic point

$$\partial_x \boldsymbol{I} = \boldsymbol{M}\boldsymbol{I}, \quad x \propto -i\eta.$$

with boundary condition $x \to -i\infty$.

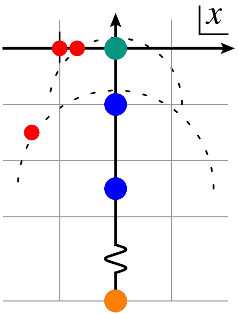

Stepping from the boundary at $x \to -i\infty$, via regular points, to the physical mass. Step size is limited by singularities of the equation.

Master integral evaluation

- Expand $\boldsymbol{I}$ around **boundary** in variable $y = x^{-1} = 0$:

$$\boldsymbol{I} = \sum_j^M \epsilon^j \sum_k^N \sum_l \boldsymbol{c}_{jkl} y^k \ln^l y + \dots$$

- Evaluate and expand around **regular points**:

$$\boldsymbol{I} = \sum_j^M \epsilon^j \sum_{k=0}^N \boldsymbol{c}_{jk} x'^k + \dots$$

- Evaluate at the **physical point.** $x = 0 \leftarrow$ **regular point**
- **Path** is fixed by **singularities** and desired precision.
- Expected relative error is $\left(\frac{\Delta}{R}\right)^N$

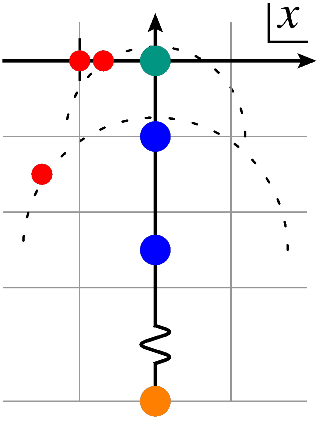

$m_W^2 \to m_W^2(1+x)$

Boundary conditions

I consider one of the master integral of the one-loop amplitude

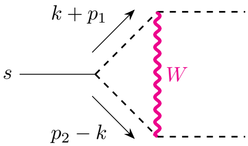

$$= \int \frac{d^d k}{(2\pi)^d} \frac{1}{(k^2-m_W^2)(k+p_1)^2(k-p_2)^2}\,.$$

As $m_W \to \infty$, we have

$m_W \gg k$

$$\frac{1}{-m_W^2}$$

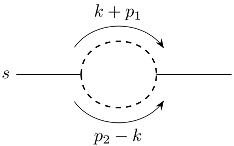

$m_W \sim k$

$$\int \frac{d^d k}{(2\pi)^d} \frac{1}{(k^2-m_W^2)(k^2)^2}$$

$$= \frac{1}{m_W^2}$$ 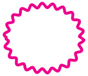 $$- \frac{1}{m_W^4}$$ 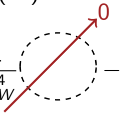 $$- \frac{1}{m_W^2} \left(\quad \right)^2$$

$$= (m_W^2)^{-\epsilon}$$ 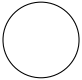

We need to consider different branch at the boundary $m_W \to \infty$

Master integral evaluation

- Some boundary conditions are known analytically *'t Hooft and Veltman 1979; Chetyrkin et al. 1980; Scharf and Tausk 1994; Gehrmann and Remiddi 2000; Gehrmann, Huber, et al. 2005*

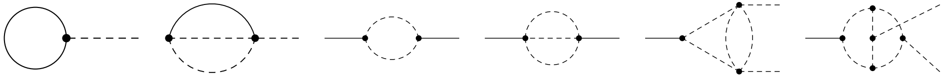

- Some are not available or not known to sufficient ϵ order:

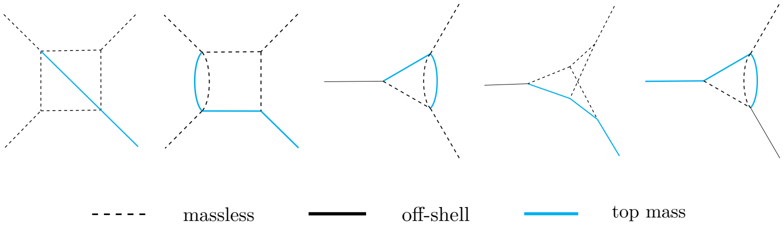

Master integral evaluation

- Add an imaginary part to the **internal top quark mass**:

$$m_t^2 \to m_t^2 - i\eta.$$

- Boundary condition: $\eta \to \infty \Rightarrow$ Physical point: $\eta \to 0$.
- Due to separation of internal and external masses, the limit $\eta \to 0$ is singular

$$\boldsymbol{I} = \sum_j^M \epsilon^j \sum_k^N \sum_l \boldsymbol{c}_{jkl} \eta^k \ln^l \eta + \dots$$

- We need to separate into branches and pick the relevant one

$$I = \eta^0 (b_{100}(\epsilon) + b_{110}(\epsilon)\eta + b_{111}(\epsilon) \ln \eta \ + \cdots) + \eta^{1-\epsilon}(b_{200} + b_{210}\eta + \cdots) + \eta^{3-4\epsilon}(\cdots)$$

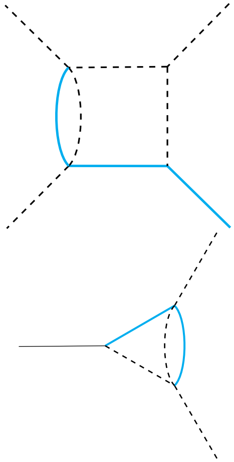

Boundary integrals

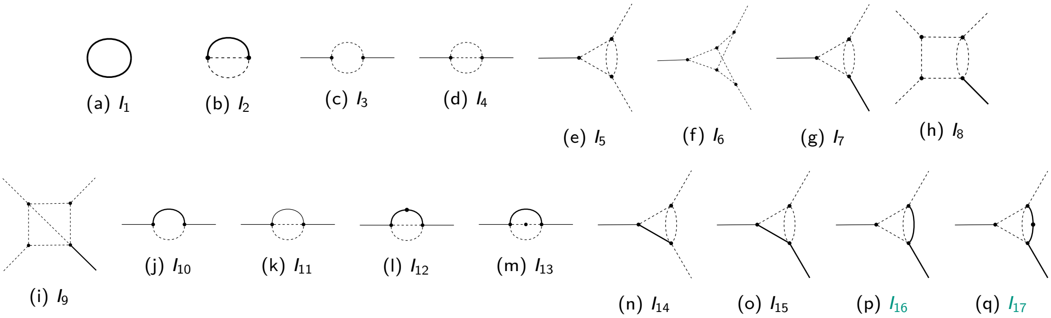

- Some boundary conditions are known analytically *'t Hooft and Veltman 1979; Chetyrkin et al. 1980; Scharf and Tausk 1994; Gehrmann and Remiddi 2000; Gehrmann, Huber, et al. 2005*
- Some are not available or are not known to sufficient order in ϵ (calculated)

Master integral evaluation

- Master integrals can be evaluated for any phase space point using differential equations in m_W^2 and m_t^2 for fixed s and t.
- We can also use the differential equations for s and t to generate phase space points.
- Solving differential equation in each direction:

$$(s_1, t_1) \xrightarrow{s} (s_2, t_1) \xrightarrow{t} (s_2, t_2)$$

- Also provides a consistency check.
- A subset of integrals were checked against `pySecDec` *Borowka, Heinrich, Jahn, Jones, Kerner, Schlenk, and Zirke 2018; Borowka, Heinrich, Jahn, Jones, Kerner, and Schlenk 2019.*

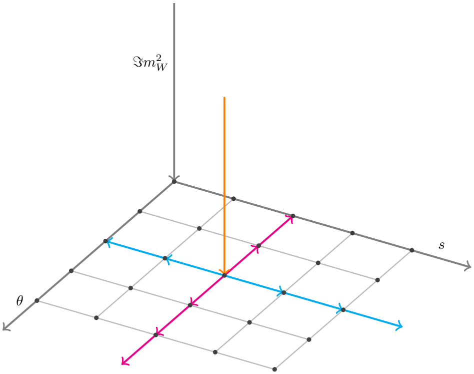

All **428** master integrals evaluated numerically to 20 digits in $\sim$ 30 minutes on a single core.

Double-virtual contribution

Karlsruhe Institute of Technology

- Comparison of poles at a typical phase space point $s \approx 104.337$ GeV^2 and $t \approx -5179.68$ GeV^2.

	ϵ^{-2}	ϵ^{-1}
$\langle \mathcal{A}^{(0)} \vert \mathcal{A}^{(2)}_{\rm nf} \rangle$	$-229.0940408654660 - 8.978163333241640i$	$-301.180298894476 4 - 264.1773596529505i$
IR poles	$-229.0940408654665 - 8.978163333241973i$	$-301.1802988944791 - 264.1773596529535i$

- The cross-section is evaluated with a **Vegas integrator**.
- 10 sets of 10^4 points extracted from a grid prepared **on the Born squared amplitude.**
- The 10 different sets give an estimation of the error on σ_{VV}: $\mathcal{O}(2\%)$ *Brønnum-Hansen, Melnikov, Quarroz, Wang, 2021*

Results

Karlsruhe Institute of Technology

- The non-factorisable correction to the leading-order cross section at 13 TeV and $\mu_F = m_t$

$$\frac{\sigma_{pp\to X+t}}{1\,\mathrm{pb}} = 117.96 + 0.26\left(\frac{\alpha_s(\mu_R)}{0.108}\right)^2$$

- *Non-factorisable* correction is about $\mathbf{0.22^{-0.04}_{+0.05}}$% for $\boldsymbol{\mu_R = m_t}$.
- *Non-factorisable* corrections **appear for the first time** at NNLO ; for this reason, they are **independent** of LO, NLO, and NNLO *factorisable* contribution. $\rightarrow$ No indication of a good scale choice.
- At $\mu_R = 40$ GeV, typical transverse momentum of the top quark, corrections become **close to 0.35%.**
- In comparison, NNLO **factorisable correction** to NLO cross section are about **0.7%** *Campbell, Neumann, et al. 2021*

Top-quark transverse momentum distribution

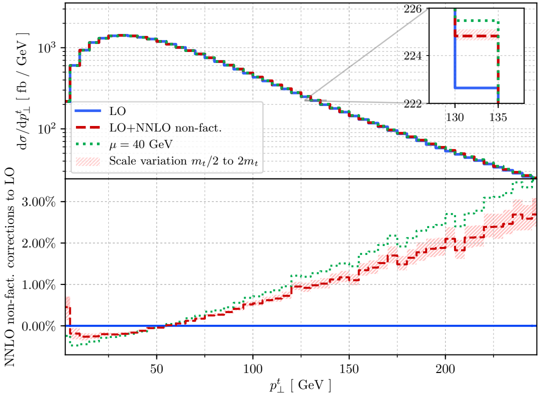

Figure: The top quark transverse momentum distribution.

- There is a **significant** $p_\perp^t$-dependence of the non-factorisable corrections.
- Non-factorisable corrections vanish around 50 GeV. The factorisable corrections vanish around 30 GeV. *Campbell, Neumann, et al. 2021*
- In some part of the phase space at low $p_\perp^t$, at the peak of the distribution, non-factorisable corrections are **dominant** compared to factorisable corrections.

Conclusion

- We computed **the missing part** of NNLO QCD corrections to the t-channel single-top production: **the non-factorisable corrections**.

- **The auxiliary mass flow method** has been used for integrals evaluation. It is sufficiently **robust** to produce results relevant for phenomenology.

- Non-factorisable corrections are smaller than, but **quite comparable** to, the factorisable ones.

- If a percent precision in single-top studies can be reached, **the non-factorisable effect will have to be taken into account.**

Thank you for your attention !

References I

't Hooft, Gerard and M. J. G. Veltman (1979). "Scalar One Loop Integrals". In: *Nucl. Phys. B* 153, pp. 365–401.

Chetyrkin, K. G., A. L. Kataev, and F. V. Tkachov (1980). "New Approach to Evaluation of Multiloop Feynman Integrals: The Gegenbauer Polynomial x Space Technique". In: *Nucl. Phys. B* 174, pp. 345–377.

Scharf, R. and J. B. Tausk (1994). "Scalar two loop integrals for gauge boson selfenergy diagrams with a massless fermion loop". In: *Nucl. Phys. B* 412, pp. 523–552.

Catani, Stefano (1998). "The Singular behavior of QCD amplitudes at two loop order". In: *Phys. Lett. B* 427, pp. 161–171. arXiv: hep-ph/9802439.

Gehrmann, T. and E. Remiddi (2000). "Differential equations for two loop four point functions". In: *Nucl. Phys. B* 580, pp. 485–518. arXiv: hep-ph/9912329.

Harris, B. W. et al. (2002). "The Fully Differential Single Top Quark Cross-Section in Next to Leading Order QCD". In: *Phys. Rev. D* 66, p. 054024. arXiv: hep-ph/0207055.

Campbell, John M., R. Keith Ellis, and Francesco Tramontano (2004). "Single top production and decay at next-to-leading order". In: *Phys. Rev. D* 70, p. 094012. arXiv: hep-ph/0408158.

Sullivan, Zack (2004). "Understanding single-top-quark production and jets at hadron colliders". In: *Phys. Rev. D* 70, p. 114012. arXiv: hep-ph/0408049.

Cao, Qing-Hong and C. -P. Yuan (2005). "Single top quark production and decay at next-to-leading order in hadron collision". In: *Phys. Rev. D* 71, p. 054022. arXiv: hep-ph/0408180.

Gehrmann, T., T. Huber, and D. Maitre (2005). "Two-loop quark and gluon form-factors in dimensional regularisation". In: *Phys. Lett. B* 622, pp. 295–302. arXiv: hep-ph/0507061.

Sullivan, Zack (2005). "Angular correlations in single-top-quark and Wjj production at next-to-leading order". In: *Phys. Rev. D* 72, p. 094034. arXiv: hep-ph/0510224.

References II

Beccaria, M. et al. (2006). “Single top production in the t-channel at LHC: A Realistic test of electroweak models”. In: *Phys. Rev. D* 74, p. 013008. arXiv: hep-ph/0605108.

Becher, Thomas and Matthias Neubert (2009). “On the Structure of Infrared Singularities of Gauge-Theory Amplitudes”. In: *JHEP* 06. [Erratum: JHEP 11, 024 (2013)], p. 081. arXiv: 0903.1126 [hep-ph].

Schwienhorst, Reinhard et al. (2011). “Single top quark production and decay in the *t*-channel at next-to-leading order at the LHC”. In: *Phys. Rev. D* 83, p. 034019. arXiv: 1012.5132 [hep-ph].

Manteuffel, A. von and C. Studerus (Jan. 2012). “Reduze 2 - Distributed Feynman Integral Reduction”. In: arXiv: 1201.4330 [hep-ph].

Assadsolimani, M. et al. (2014). “Calculation of two-loop QCD corrections for hadronic single top-quark production in the *t* channel”. In: *Phys. Rev. D* 90.11, p. 114024. arXiv: 1409.3654 [hep-ph].

Czakon, M. and D. Heymes (2014). “Four-dimensional formulation of the sector-improved residue subtraction scheme”. In: *Nucl. Phys. B* 890, pp. 152–227. arXiv: 1408.2500 [hep-ph].

Borowka, S., G. Heinrich, S. Jahn, S. P. Jones, M. Kerner, J. Schlenk, and T. Zirke (2018). “pySecDec: a toolbox for the numerical evaluation of multi-scale integrals”. In: *Comput. Phys. Commun.* 222, pp. 313–326. arXiv: 1703.09692 [hep-ph].

Liu, Xiao, Yan-Qing Ma, and Chen-Yu Wang (2018). “A Systematic and Efficient Method to Compute Multi-loop Master Integrals”. In: *Phys. Lett. B* 779, pp. 353–357. arXiv: 1711.09572 [hep-ph].

Borowka, S., G. Heinrich, S. Jahn, S. P. Jones, M. Kerner, and J. Schlenk (2019). “A GPU compatible quasi-Monte Carlo integrator interfaced to pySecDec”. In: *Comput. Phys. Commun.* 240, pp. 120–137. arXiv: 1811.11720 [physics.comp-ph].

References III

Liu, Tao, Kirill Melnikov, and Alexander A. Penin (2019). “Nonfactorizable QCD Effects in Higgs Boson Production via Vector Boson Fusion”. In: *Phys. Rev. Lett.* 123.12, p. 122002. arXiv: 1906.10899 [hep-ph].

Klappert, Jonas and Fabian Lange (2020). “Reconstructing rational functions with FireFly”. In: *Comput. Phys. Commun.* 247, p. 106951. arXiv: 1904.00009 [cs.SC].

Klappert, Jonas, Fabian Lange, et al. (Aug. 2020). “Integral Reduction with Kira 2.0 and Finite Field Methods”. In: arXiv: 2008.06494 [hep-ph].

Liu, Xiao, Yan-Qing Ma, Wei Tao, et al. (Sept. 2020). “Calculation of Feynman loop integration and phase-space integration via auxiliary mass flow”. In: arXiv: 2009.07987 [hep-ph].

Campbell, John, Tobias Neumann, and Zack Sullivan (2021). “Single-top-quark production in the t-channel at NNLO”. In: *JHEP* 02, p. 040. arXiv: 2012.01574 [hep-ph].

Klappert, Jonas, Sven Yannick Klein, and Fabian Lange (2021). “Interpolation of dense and sparse rational functions and other improvements in FireFly”. In: *Comput. Phys. Commun.* 264, p. 107968. arXiv: 2004.01463 [cs.MS].

Liu, Xiao and Yan-Qing Ma (July 2021). “Multiloop corrections for collider processes using auxiliary mass flow”. In: arXiv: 2107.01864 [hep-ph].

Non-factorisable contributions at NNLO

- What is needed to compute non-factorisable contribution at NNLO ?

$$d\hat{\sigma}^{\text{NNLO}}_{\text{n.f.}} = \underbrace{d\hat{\sigma}_{\text{RR}}}_{\mathcal{A}_6^{(0)}} + \underbrace{d\hat{\sigma}_{\text{RV}}}_{\mathcal{A}_5^{(1)},\,\mathcal{A}_5^{(0)}} + \underbrace{d\hat{\sigma}_{\text{VV}}}_{\mathcal{A}_4^{(2)},\,\mathcal{A}_4^{(1)},\,\mathcal{A}_4^{(0)}}$$

$$d\hat{\sigma}_{\text{RR}} : \mathcal{A}_6^{(0)} \otimes \mathcal{A}_6^{(0)} =$$

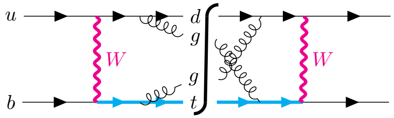

$$d\hat{\sigma}_{\text{RV}} : \mathcal{A}_5^{(1)} \otimes \mathcal{A}_5^{(0)} =$$

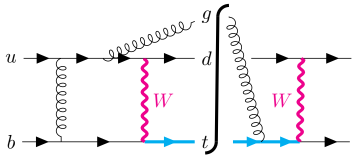

Non-factorisable contributions at NNLO

- What is needed to compute non-factorisable contribution at NNLO ?

$$d\hat{\sigma}^{\text{NNLO}}_{\text{n.f.}} = \underbrace{d\hat{\sigma}_{\text{RR}}}_{\mathcal{A}_6^{(0)}} + \underbrace{d\hat{\sigma}_{\text{RV}}}_{\mathcal{A}_5^{(1)},\, \mathcal{A}_5^{(0)}} + \underbrace{d\hat{\sigma}_{\text{VV}}}_{\mathcal{A}_4^{(2)},\, \mathcal{A}_4^{(1)},\, \mathcal{A}_4^{(0)}}$$

$$d\hat{\sigma}_{\text{RR}} : \mathcal{A}_6^{(0)} \otimes \mathcal{A}_6^{(0)} =$$

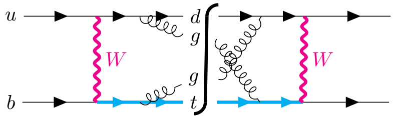

$$d\hat{\sigma}_{\text{RV}} : \mathcal{A}_5^{(1)} \otimes \mathcal{A}_5^{(0)} =$$

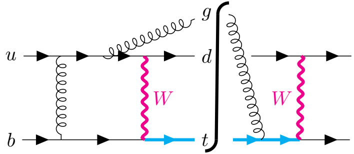

Master integral evaluation

- Master integrals can be evaluated for any phase space point using differential equations in m_W^2 and m_t^2 for fixed s and t.
- We can also use the differential equations for s and t to generate phase space points.
- Solving differential equation in each direction:

$$(s_1, t_1) \xrightarrow{s} (s_2, t_1) \xrightarrow{t} (s_2, t_2)$$

- Also provides a consistency check.
- A subset of integrals were checked against `pySecDec` *Borowka, Heinrich, Jahn, Jones, Kerner, Schlenk, and Zirke 2018; Borowka, Heinrich, Jahn, Jones, Kerner, and Schlenk 2019.*

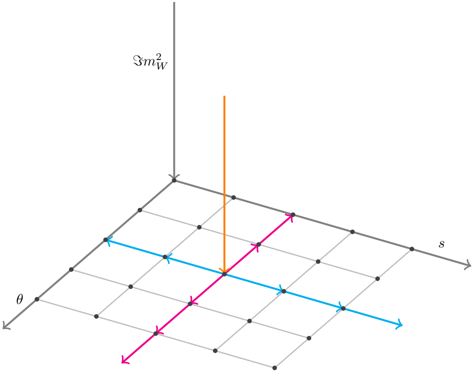

Master integral evaluation

- Some boundary conditions are known analytically *'t Hooft and Veltman 1979; Chetyrkin et al. 1980; Scharf and Tausk 1994; Gehrmann and Remiddi 2000; Gehrmann, Huber, et al. 2005*

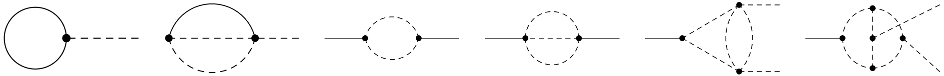

- Some are not available or not known to sufficient ϵ order:

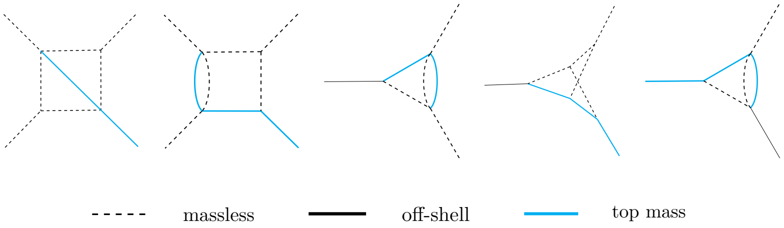

How to extract the soft singularity from loop amplitudes?

It is standard to project out loop amplitudes on **colour space vectors** $|c\rangle$ to extract their singularities *Catani 1998*

$$\langle c|\mathcal{A}_4^{(1)}(1_q,2_b,3_{q'},4_t)\rangle = \frac{\alpha_s}{2\pi}\left(\cdots + t^a_{c_3c_1}t^a_{c_4c_2}\,B_1(1_q,2_b,3_{q'},4_t)\right)\,.$$

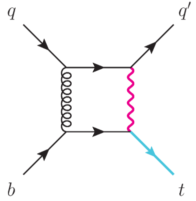

The **pole structure** of the one-loop amplitude reads

$$B_1(1_q,2_b,3_{q'},4_t) = I_1(\epsilon)\,A_0(1_q,2_b,3_{q'},4_t) + B_{1,\mathrm{fin}}(1_q,2_b,3_{q'},4_t)\,,$$

where

$$I_1(\epsilon) \equiv \frac{1}{\epsilon}\left[\ln\left(\frac{p_1\cdot p_4\;p_2\cdot p_3}{p_1\cdot p_2\;p_3\cdot p_4}\right) + 2\pi i\right]\,.$$

The **Abelian nature** of the *non-factorisable* corrections leads to a simple pole structure of the two-loop amplitude

$$B_2(1_q,2_b,3_{q'},4_t) = -\frac{I_1^2(\epsilon)}{2}\,A_0(1_q,2_b,3_{q'},4_t) + I_1(\epsilon)\,B_1(1_q,2_b,3_{q'},4_t) + B_{2,\mathrm{fin}}(1_q,2_b,3_{q'},4_t)\,.$$

How to extract the soft singularity from real emission?

We consider one gluon emission amplitude and extract the **color structure**

$$\langle c|\mathcal{A}_5^{(0)}(1_q,2_b,3_{q'},4_t,5_g)\rangle = g_s\left(t^{c_5}_{c_3c_1}\delta_{c_4c_2}\,A_0^L(1_q,2_b,3_{q'},4_t;5_g)+\delta_{c_3c_1}t^{c_5}_{c_4c_2}\,A_0^H(1_q,2_b,3_{q'},4_t;5_g)\right),$$

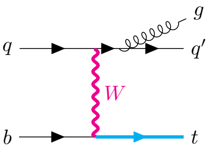

The amplitude **factorises** in the limit where the gluon energy $E_5 \to 0$

$$S_5 A_0^L = J(3,1;5,\epsilon_5)A_0(1_q,2_b,3_{q'},4_t) \quad \text{with} \quad J(i,j;k,\epsilon)=\epsilon_\mu\left(\frac{p_i^\mu}{p_i\cdot p_k}-\frac{p_j^\mu}{p_j\cdot p_k}\right)$$

We need the **interference** between emission from the **light line** A_0^L and the one with emission from **heavy line** A_0^H

$$S_5\left\{2\mathrm{Re}[A_0^{L*}A_0^H]\right\}=\sum_\lambda J(3,1,5,\epsilon_5)J(4,2,5,\epsilon_5)|A_0(1_q,2_b,3_{q'},4_t)| = \mathrm{Eik}_{nf}(1_q,2_b,3_{q'},4_t,5_g)|A_0(1_q,2_b,3_{q'},4_t)|$$

After integration over the gluon phase space

$$g_s^2\int[dk]\,\mathrm{Eik}_{\mathrm{nf}}(1_q,2_b,3_{q'},4_t;k_g)\equiv\frac{\alpha_s}{2\pi}\left(\frac{2E_{\max}}{\mu}\right)^{-2\epsilon}\left[\frac{1}{\epsilon}\ \ln\left(\frac{p_1\cdot p_4\ p_2\cdot p_3}{p_1\cdot p_2\ p_3\cdot p_4}\right)+\mathcal{O}(\epsilon^0)\right].$$

Master integral evaluation

- Add an imaginary part to the **internal top quark mass**:

$$m_t^2 \to m_t^2 - i\eta.$$

- Boundary condition: $\eta \to \infty \Rightarrow$ Physical point: $\eta \to 0$.
- Due to separation of internal and external masses, the limit $\eta \to 0$ is singular

$$\boldsymbol{I} = \sum_j^M \epsilon^j \sum_k^N \sum_l \boldsymbol{c}_{jkl} \eta^k \ln^l \eta + \dots$$

- We need to separate into branches and pick the relevant one

$$I = \eta^0 (b_{100}(\epsilon) + b_{110}(\epsilon)\eta + b_{111}(\epsilon) \ln \eta \; + \cdots) + \eta^{1-\epsilon}(b_{200} + b_{210}\eta + \cdots) + \eta^{3-4\epsilon}(\cdots)$$

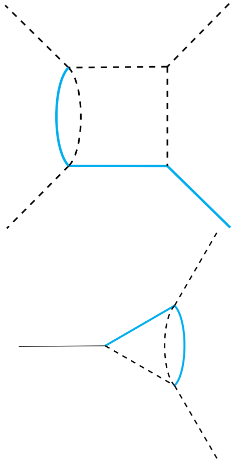

Master integral evaluation

- Simple boundary conditions for internal $m_t \to \infty$

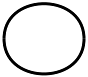

(a) I_1

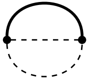

(b) I_2

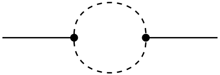

(c) I_3

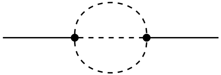

(d) I_4

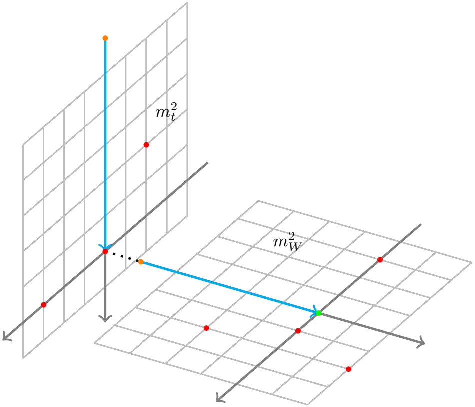

Real-virtual contribution

We need the one-loop five-point amplitude $\mathcal{A}_5^{(1)}(1_q, 2_b, 2_{q'}, 4_t, 5_g)$.

- Turn out to be **non-trivial** due to the presence of **multiple mass scales**!
- 24 diagrams generated with `QGRAF` and `FORM` - 8 pentagons and 16 boxes

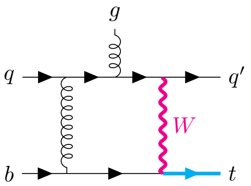

7 mass scales

Spinor structure - How to extract ϵ dependence?

External momenta lives in $d = 4$, internal momenta in $d = 4-2\epsilon$: $\gamma^\mu = \gamma^{\bar{\mu}} + \gamma^{\tilde{\mu}}$

$$\overline{u}_t(p_4)\gamma^\mu\gamma^\nu u_b(p_2) = \overline{u}_t(p_4)\gamma^{\bar{\mu}}\gamma^{\bar{\nu}} u_b(p_2) + g^{\tilde{\mu}\tilde{\nu}}\,\overline{u}_t(p_4)u_b(p_2)\,.$$

W boson **forces light quark to be left-handed** and we decompose the massive momentum into 2 massless momenta

$$P_L u(p_4) = |4^\flat] + \frac{m_t}{\langle 4^\flat 1_q\rangle}|1_q\rangle, \qquad P_R u(p_4) = |4^\flat\rangle + \frac{m_t}{[4^\flat 1_q]}|1_q]$$

We are left with 2 spinor structures per helicity configuration

E.g. Left-handed gluon and left-handed top: $\langle 4^\flat 5_g\rangle^2 \langle 1_q 3_{q'}\rangle [4^\flat 1_q] [1_q 2_b]$, $\langle 4^\flat 5_g\rangle \langle 3_{q'} 5_g\rangle [1_q 2_b]$

References

Form factors

Reduction of pentagons of rank r, $r \leq 3$

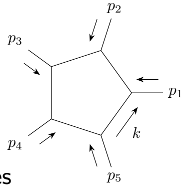

$$\int \frac{d^d k}{(2\pi)^d} \frac{k^{\mu_1} \dots k^{\mu_r}}{\prod_{i=1}^{5} [(k+q_i)^2 - m_i^2]} \quad \text{where } q_i = \sum_{j=1}^{i} p_j$$

We introduce the **van Neerven-Vermaseren basis** $v_i \cdot p_j = \delta_{ij}$ and the loop momentum becomes

$$k^\mu = \sum_{i=1}^{4} (k \cdot p_i) v_i$$

and rewrite $$k \cdot p_i = \underbrace{\frac{1}{2}\left[(k+q_i)^2 - m_i^2\right] - \frac{1}{2}\left[(k+q_{i-1})^2 - m_{i-1}^2\right]}_{\text{Boxes of rank } r-1 \quad \to \text{Passarino-Veltman}} + \underbrace{\frac{1}{2}\left[m_i^2 - m_{i-1}^2 - p_i^2 - 2p_i \cdot q_{i-1}\right]}_{\text{Pentagon of rank } r-1 \quad \to \text{Repeat}}$$

Scalar pentagon can be expressed as a combination of boxes up to $\mathcal{O}(\epsilon)$

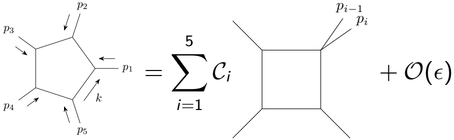

Numerical stability

Karlsruhe Institute of Technology

- The real-virtual amplitude can be written in terms of **109** scalar box,triangle and bubble integrals.
- By switching to a basis with **finite box integrals**, the complexity of the integral coefficient **reduces drastically**.

$$\text{e.g.} \qquad I_{4,1} = \int \frac{\mathrm{d}^d k}{(2\pi)^d} \frac{1}{k^2(k-p_1)^2(k-p_1-p_2)^2(k-p_1-p_2+p_5)^2} \, .$$

This integral is **infrared-divergent** when one of the propagator goes on-shell. We can **regulate** these divergences through numerator insertion

$$\begin{aligned} \mathrm{tr}\left((-\not{p}_1)(\not{k}-\not{p}_1)(\not{k}-\not{p}_1-\not{p}_2)(\not{p}_5)\right) = & - s_{12}\left(s_{12}+s_{15}-s_{34}\right) + \left(s_{12}+s_{15}-s_{34}\right) k^2 \\ & - \left(s_{12}-s_{34}\right)(k-p_1)^2 + \left(s_{12}+s_{15}\right)(k-p_1-p_2)^2 \\ & - s_{12}\,(k-p_1-p_2+p_5)^2 \, . \end{aligned}$$

After this change of basis:

- The **complicated coefficients** in front of the box integrals can be evaluated with $\epsilon \to 0$.
- The coefficients of the triangle integrals either become independent of $d = 4 - 2\epsilon$ or simply **vanish**.

Leading jet rapidity distribution

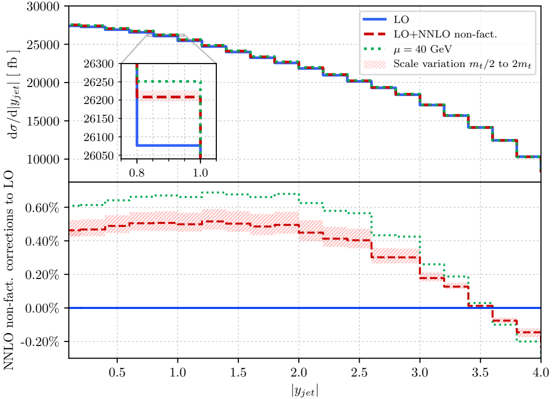

Figure: Rapidity of the leading jet distribution.

- k_t jet algorithm - $p_\perp^{jet} = 30\,\mathrm{GeV}$ and $R_{jet} = 0.4$
- Constant correction of $\mathcal{O}(0.5\%)$ from $|y_{jet}| < 2$.
- Corrections change sign at $|y_{jet}| \sim 3.5$.

Table for factorisable corrections

	7 TeV pp		14 TeV pp		1.96 TeV $\bar{p}p$
	top	anti-top	top	anti-top	$t+\bar{t}$
$\sigma_{\rm LO}^{\mu=m_t}$	$37.1^{+7.1\%}_{-9.5\%}$	$19.1^{+7.3\%}_{-9.7\%}$	$134.6^{+10.0\%}_{-12.1\%}$	$78.9^{+10.4\%}_{-12.6\%}$	$2.09^{+0.8\%}_{-3.1\%}$
$\sigma_{\rm LO}^{\rm DDIS}$	$39.5^{+6.4\%}_{-8.6\%}$	$19.9^{+7.0\%}_{-9.3\%}$	$140.9^{+9.4\%}_{-11.4\%}$	$80.7^{+10.2\%}_{-12.3\%}$	$2.31^{-0.3\%}_{-1.8\%}$
$\sigma_{\rm NLO}^{\mu=m_t}$	$41.4^{+3.0\%}_{-2.0\%}$	$21.5^{+3.1\%}_{-2.0\%}$	$154.3^{+3.1\%}_{-2.3\%}$	$91.4^{+3.1\%}_{-2.2\%}$	$1.96^{+3.1\%}_{-2.3\%}$
$\sigma_{\rm NLO}^{\rm DDIS}$	$41.8^{+3.3\%}_{-2.0\%}$	$21.5^{+3.4\%}_{-1.6\%}$	$154.4^{+3.7\%}_{-1.4\%}$	$91.2^{+3.1\%}_{-1.8\%}$	$2.00^{+3.6\%}_{-3.4\%}$
	PDF $^{+1.7\%}_{-1.4\%}$	PDF $^{+2.2\%}_{-1.5\%}$	PDF $^{+1.7\%}_{-1.1\%}$	PDF $^{+1.9\%}_{-0.9\%}$	PDF $^{+4.3\%}_{-5.3\%}$
$\sigma_{\rm NNLO}^{\mu=m_t}$	$41.9^{+1.2\%}_{-0.7\%}$	$21.9^{+1.2\%}_{-0.7\%}$	$153.3(2)^{+1.0\%}_{-0.6\%}$	$91.5(2)^{+1.1\%}_{-0.9\%}$	$2.08^{+2.0\%}_{-1.3\%}$
$\sigma_{\rm NNLO}^{\rm DDIS}$	$41.9^{+1.3\%}_{-0.8\%}$	$21.8^{+1.3\%}_{-0.7\%}$	$153.4(2)^{+1.1\%}_{-0.7\%}$	$91.2(2)^{+1.1\%}_{-0.9\%}$	$2.07^{+1.7\%}_{-1.1\%}$
	PDF $^{+1.3\%}_{-1.1\%}$	PDF $^{+1.4\%}_{-1.3\%}$	PDF $^{+1.2\%}_{-1.0\%}$	PDF $^{+1.0\%}_{-1.0\%}$	PDF $^{+3.7\%}_{-5.0\%}$

Figure: Fully inclusive in pb for pp at 7 TeV and 14 TeV (LHC), as well as $p\bar{p}$ at 1.96 TeV (Tevatron) with scales $\mu_R = \mu_F = m_t$ and DDIS scales and using CT14 PDFs. *Campbell, Neumann, et al. 2021*

Results for the virtual contribution

- Comparison of poles at a typical phase space point $s \approx 104.337$ GeV^2 and $t \approx -5179.68$ GeV^2.

	ϵ^{-2}	ϵ^{-1}
$\langle \mathcal{A}^{(0)} \vert \mathcal{A}_{\rm nf}^{(2)} \rangle$	$-229.0940408654660 - 8.978163333241640i$	$-301.1802988944764 - 264.1773596529505i$
IR poles	$-229.0940408654665 - 8.978163333241973i$	$-301.1802988944791 - 264.1773596529535i$

- Double-virtual cross-section calculation from fixed grid of 100k points

$$\sigma^{ub}_{pp\to dt} = \left(90.3 + 0.3\left(\frac{\alpha_s(\mu_{\rm nf})}{0.108}\right)^2\right) \text{ pb}$$

- Correction of about 0.3% for $\mu_{\rm nf} = 173$ GeV

- **Typical transverse momentum**: $\mu_{nf} = 40 - 60$ GeV. The magnitude of the non-factorisable corrections will **increase** by a factor $\mathcal{O}(1.5)$ and become close to **half a percent**.

Spinor structures and γ_5

- Projection on to 11 spinor stuctures *Assadsolimani et al. 2014*

$$
\begin{aligned}
S_1 &= \bar{t}(p_4)\; b(p_2) \times \bar{q}'(p_3)\, \not{p}_4\, b(p_1) \\
S_2 &= \bar{t}(p_4)\, \not{p}_1\, b(p_2) \times \bar{q}'(p_3)\, \not{p}_4\, b(p_1) \\
S_3 &= \bar{t}(p_4)\, \gamma^{\mu_1}\, b(p_2) \times \bar{q}'(p_3)\, \gamma_{\mu_1}\, b(p_1) \\
S_4 &= \bar{t}(p_4)\, \gamma^{\mu_1} \not{p}_1\, b(p_2) \times \bar{q}'(p_3)\, \gamma_{\mu_1}\, b(p_1) \\
&\;\;\vdots \\
S_{11} &= \bar{t}(p_4)\, \gamma^{\mu_1}\gamma^{\mu_2}\gamma^{\mu_3}\gamma^{\mu_4}\gamma^{\mu_5}\, b(p_2) \times \bar{q}'(p_3)\, \gamma_{\mu_1}\gamma_{\mu_2}\gamma_{\mu_3}\gamma_{\mu_4}\gamma_{\mu_5}\, b(p_1)
\end{aligned}
$$

- Exploit anti-commutativity of γ_5 to move left-handed projectors to external *massless* fermions.
- Non-factorisable amplitude is expressed in terms of 11 form factors $\mathcal{A}_{nf}^{(2)} = \vec{f} \cdot \vec{S}$
- Form factors does not depend on helicities of external states.
  $\rightarrow$ **one can compute them with vector currents**.

Helicity amplitudes

- *'t Hooft-Veltman scheme*: external momenta in $d = 4$ and internal in $d = 4 - 2\epsilon$
- *At least two* matrices in $d = 4 - 2\epsilon$ are needed between two $d = 4$ spinors to have a support in -2ϵ space.

$$\bar{u}_d(p_3)\gamma_\mu\gamma_\nu \not{p}_4 u_u(p_1) \to \begin{pmatrix} \bar{u}_d(p_3) \\ 0 \end{pmatrix} \begin{pmatrix} \underbrace{\gamma_\mu}_{d=4} & 0 \\ 0 & \underbrace{\gamma_\mu}_{d=-2\epsilon} \end{pmatrix} \begin{pmatrix} \underbrace{\gamma_\nu}_{d=4} & 0 \\ 0 & \underbrace{\gamma_\nu}_{d=-2\epsilon} \end{pmatrix} \begin{pmatrix} \underbrace{\not{p}_4}_{d=4} & 0 \\ 0 & \underbrace{0}_{d=-2\epsilon} \end{pmatrix} \begin{pmatrix} \bar{u}_u(p_1) \\ 0 \end{pmatrix}$$

- ϵ dependence can be explicitly and unambigously extracted and γ_5 restored

$$\begin{cases} \mathcal{S}_{1,..,4} = \mathcal{S}^{(4)}_{1,..,4}\,, \\ \mathcal{S}_{5,6} = \mathcal{S}^{(4)}_{5,6} - 2\epsilon\mathcal{S}^{(4)}_{1,2}\,, \\ \mathcal{S}_{7,8} = \mathcal{S}^{(4)}_{7,8} - 6\epsilon\mathcal{S}^{(4)}_{3,4}\,, \\ \mathcal{S}_{9,10} = \mathcal{S}^{(4)}_{9,10} - 12\epsilon\mathcal{S}^{(4)}_{5,6} + \left(12\epsilon^2 + 4\epsilon\right)\mathcal{S}^{(4)}_{1,2}\,, \\ \mathcal{S}_{11} = \mathcal{S}^{(4)}_{11} - 20\epsilon\mathcal{S}^{(4)}_{7} + \left(60\epsilon^2 + 20\epsilon\right)\mathcal{S}^{(4)}_{3} \end{cases}$$

IBP reduction

- Find symmetry relations with `REDUZE` 2 *Manteuffel and Studerus 2012.*
- Reduction performed **analytically** with `KIRA` 2.0: *Klappert, Lange, et al. 2020* and `FireFly` *Klappert and Lange 2020; Klappert, Klein, et al. 2021:*

$$\langle A^{(0)} | A^{(2)}_{\mathrm{nf}} \rangle = \sum_{i=1}^{428} c_i(d, s, t, m_t, m_W) I_i$$

- Analytic reduction is possible with four scales $(s,\ t,\ m_t,\ m_W)$: $\mathcal{O}(1)$ day
- 428 master integrals I_i in 18 families
- file size of the simplified coefficients c_i: $\mathcal{O}(1)$ MB

Master integrals evaluation

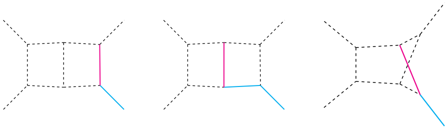

- Based on the **auxiliary mass flow method** *Liu, Ma, and Wang 2018; Liu, Ma, Tao, et al. 2020; Liu and Ma 2021*

$$m_W^2 \to m_W^2 - i\eta.$$

- Solve differential equations at each kinematic point

$$\partial_x \boldsymbol{I} = \boldsymbol{M}\boldsymbol{I}, \quad x \propto -i\eta.$$

with boundary condition $x \to -i\infty$.

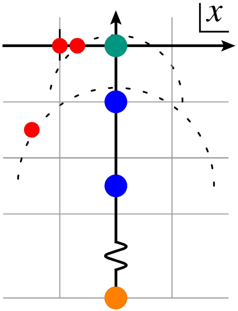

Stepping from the boundary at $x \to -i\infty$, via regular points, to the physical mass. Step size is limited by singularities of the equation.

Master integral evaluation

- Expand $\boldsymbol{I}$ around **boundary** in variable $y = x^{-1} = 0$:

$$\boldsymbol{I} = \sum_{j}^{M} \epsilon^{j} \sum_{k}^{N} \sum_{l} c_{jkl} y^{k} \ln^{l} y + \dots$$

- Evaluate and expand around **regular points**:

$$\boldsymbol{I} = \sum_{j}^{M} \epsilon^{j} \sum_{k=0}^{N} c_{jk} x'^{k} + \dots$$

- Evaluate at the **physical point.** $x = 0 \leftarrow$ **regular point**
- **Path** is fixed by **singularities** and desired precision.

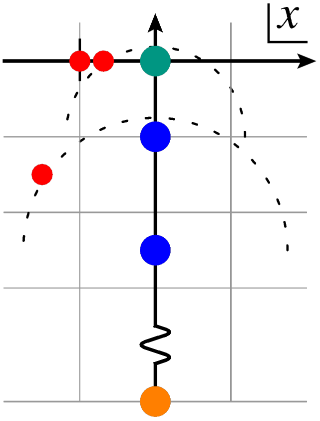

$m_W^2 \to m_W^2(1+x)$

Boundary conditions

- Most of the integrals needed can be found in the literature.
- Some of them are not available or are not known to sufficiently high ϵ order.
- All **428** master integrals evaluated numerically to 20 digits in ~ 30 minutes on a single core.

Master integrals for the boundary conditions

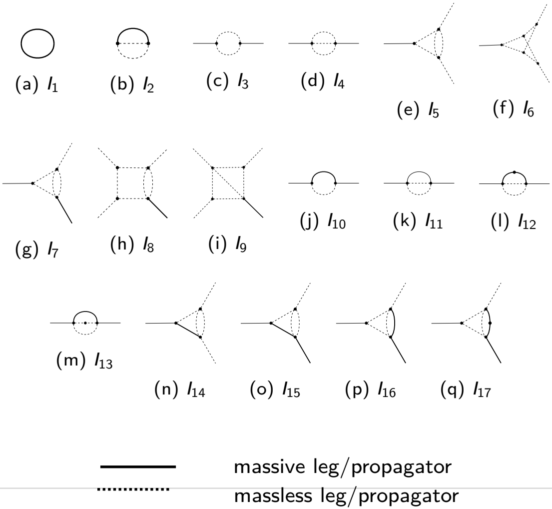

Master integral evaluation

- We can use the differential equation w.r.t s and t to generate phase space points.
- Solving differential equation in each direction:

$$(s_1, t_1) \xrightarrow{s} (s_2, t_1) \xrightarrow{t} (s_2, t_2)$$

- This also serves as a consistency check.

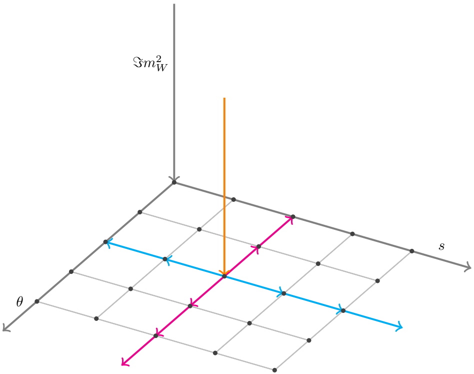

Evaluation of the cross-section

- The cross-section is evaluated with the help of a **Vegas integrator**.
- 10 grids of 10^4 points are prepared **on the Born squared amplitude**.
- $\mathcal{A}^{(1)}_{nf} \otimes \mathcal{A}^{(1)}_{nf}$ and $\mathcal{A}^{(0)} \otimes \mathcal{A}^{(2)}_{nf}$ are evaluated for each of the 10^5 points. ($\approx \mathcal{O}(1$ day$)$)
- The 10 different set of points give an estimation of the error of the total cross-section. (2%)

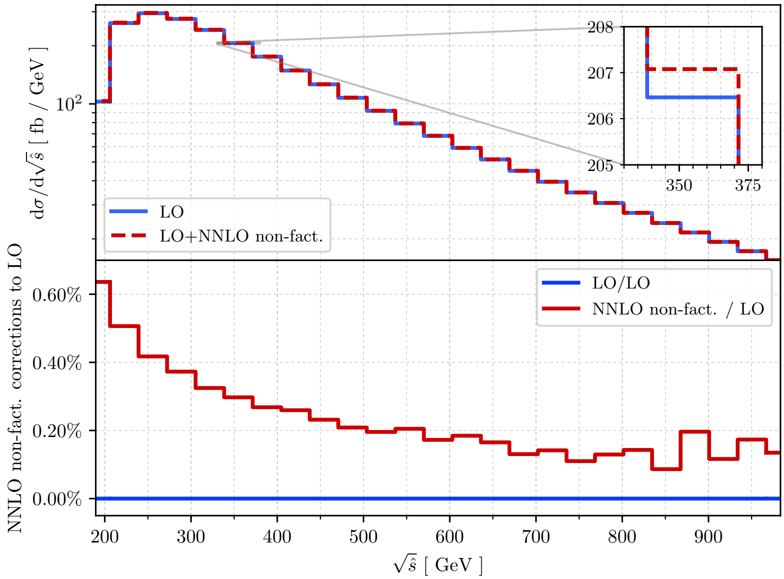

$d\sigma/d\sqrt{\hat{s}}$ [fb / GeV]
10^2
LO
LO+NNLO non-fact.
208
207
206
205
350
375
NNLO non-fact. corrections to LO
0.60%
0.40%
0.20%
0.00%
LO/LO
NNLO non-fact. / LO
200
300
400
500
600
700
800
900
$\sqrt{\hat{s}}$ [GeV]

References

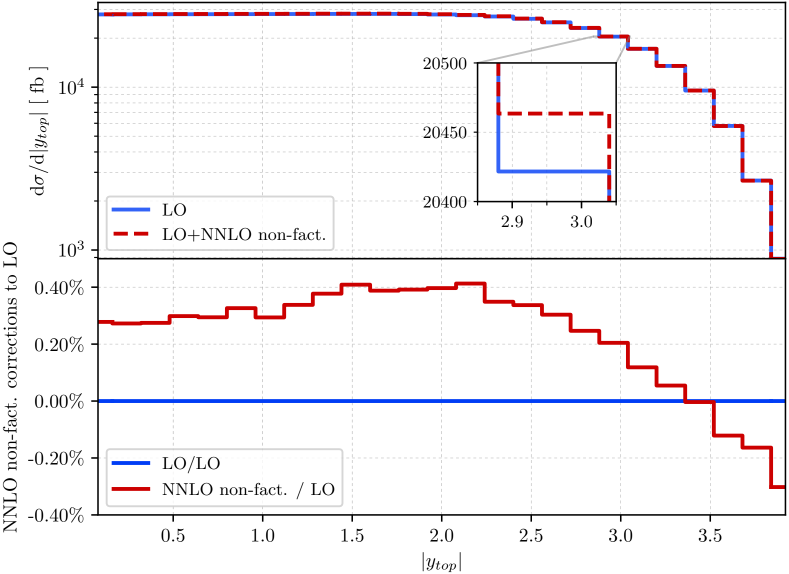

dσ/d|y_{top}| [fb]
10^4
10^3
20500
20450
20400
2.9
3.0
LO
LO+NNLO non-fact.
NNLO non-fact. corrections to LO
0.40%
0.20%
0.00%
-0.20%
-0.40%
LO/LO
NNLO non-fact. / LO
0.5
1.0
1.5
2.0
2.5
3.0
3.5
|y_{top}|

UV and IR singularities

- **No UV divergences** if we consider only non-factorisable contributions at NNLO.
- IR divergences are predicted using colour-space operators. *Catani 1998; Becher and Neubert 2009; Czakon and Heymes 2014*

$$|\mathcal{A}_{\rm nf}\rangle = \boldsymbol{Z}_{\rm nf}|\mathcal{F}_{\rm nf}\rangle, \qquad \mu\frac{d}{d\mu}\boldsymbol{Z}_{\rm nf} = -\boldsymbol{\Gamma}_{\rm nf}\boldsymbol{Z}_{\rm nf}$$

where the anomalous dimension operator, $\boldsymbol{\Gamma}_{\rm nf}$, is limited to non-factorisable relevant contributions

$$\boldsymbol{\Gamma}_{\rm nf} = \left(\frac{\alpha_s}{4\pi}\right)\boldsymbol{\Gamma}_{0,\rm nf} = \left(\frac{\alpha_s}{4\pi}\right)4\left[\boldsymbol{T}_u\cdot\boldsymbol{T}_b\ln\left(\frac{\mu^2}{-s-i\varepsilon}\right) + \boldsymbol{T}_b\cdot\boldsymbol{T}_d\ln\left(\frac{\mu^2}{-u-i\varepsilon}\right)\right.$$
$$\left. + \boldsymbol{T}_u\cdot\boldsymbol{T}_t\ln\left(\frac{\mu\, m_t}{m_t^2-u-i\varepsilon}\right) + \boldsymbol{T}_d\cdot\boldsymbol{T}_t\ln\left(\frac{\mu\, m_t}{m_t^2-s-i\varepsilon}\right)\right]$$

- Divergences of non-factorisable amplitude starts at $1/\epsilon^2$ due to **absence of collinear contributions**.

$$\langle\mathcal{A}^{(0)}|\mathcal{A}^{(2)}_{\rm nf}\rangle = -\frac{1}{8\epsilon^2}\langle\mathcal{A}^{(0)}|\boldsymbol{\Gamma}^2_{0,\rm nf}|\mathcal{A}^{(0)}\rangle + \frac{1}{2\epsilon}\langle\mathcal{A}^{(0)}|\boldsymbol{\Gamma}_{0,\rm nf}|\mathcal{A}^{(1)}_{\rm nf}\rangle + \langle\mathcal{A}^{(0)}|\mathcal{F}^{(2)}_{\rm nf}\rangle,$$
$$\langle\mathcal{A}^{(1)}_{\rm nf}|\mathcal{A}^{(1)}_{\rm nf}\rangle = \frac{1}{4\epsilon^2}\langle\mathcal{A}^{(0)}||\boldsymbol{\Gamma}_{0,\rm nf}|^2|\mathcal{A}^{(0)}\rangle + \frac{1}{2\epsilon}\langle\mathcal{A}^{(1)}_{\rm nf}|\boldsymbol{\Gamma}_{0,\rm nf}|\mathcal{A}^{(0)}\rangle + \frac{1}{2\epsilon}\langle\mathcal{A}^{(0)}|\boldsymbol{\Gamma}^\dagger_{0,\rm nf}|\mathcal{A}^{(1)}_{\rm nf}\rangle + \langle\mathcal{F}^{(1)}_{\rm nf}|\mathcal{F}^{(1)}_{\rm nf}\rangle.$$